doi.org/10.26434/chemrxiv.12121227.v1

Hydrolysis of Dimethyl Methylphosphonate (DMMP) in Hot-Compressed Water

Brian Pinkard, Shreyas Shetty, John Kramlich, Per G. Reinhall, Igor V. Novosselov

Submitted date: 14/04/2020 • Posted date: 16/04/2020

Citation information: Pinkard, Brian; Shetty, Shreyas; Kramlich, John; Reinhall, Per G.; Novosselov, Igor V. (2020): Hydrolysis of Dimethyl Methylphosphonate (DMMP) in Hot-Compressed Water. ChemRxiv. Preprint. https://doi.org/10.26434/chemrxiv.12121227.v1

Dimethyl methylphosphonate (DMMP) is widely used as a chemical surrogate for G- and V-type nerve agents, exhibiting similar physiochemical properties, yet significantly lower toxicity. Continuous hydrolysis of DMMP in hot-compressed water is performed at temperatures from 200 to 300 °C, pressures of 20 and 30 MPa, and residence times from 30 to 80 s to evaluate the effects of pressure and temperature on reaction kinetics. DMMP hydrolysis is observed to follow pseudo-first-order reaction behavior, producing methylphosphonic acid and methanol as the only detectable reaction products. This is significant for the practical implementation of a continuous hydrothermal reactor for chemical warfare agent neutralization, as the process only yields stable, less-toxic compounds. Pressure has no discernible effect on the hydrolysis rate in compressed liquid water. Pseudo-first-order Arrhenius parameters are determined, with an activation energy of 90.17±5.68 kJ mol^{-1} and a pre-exponential factor of $10^{7.51\pm0.58}$ s^{-1}.

File list (1)

DMMP Paper - ChemRXiv.pdf (0.96 MiB) view on ChemRxiv • download file

Hydrolysis of Dimethyl Methylphosphonate (DMMP) in Hot-Compressed Water

Brian R. Pinkard[a,]*, Shreyas Shetty*[a]*, John C. Kramlich*[a]*, Per G. Reinhall*[a]*, Igor V. Novosselov*[a, b]

[a] University of Washington, Mechanical Engineering Department, Seattle, WA 98195

[b] University of Washington, Institute for Nanoengineered Systems, Seattle, WA 98195

* Corresponding Author: pinkardb@uw.edu; +1 253 3105882

ORCID 0000-0002-4517-4712

Abstract

Dimethyl methylphosphonate (DMMP) is widely used as a chemical surrogate for G- and V-type nerve agents, exhibiting similar physiochemical properties, yet significantly lower toxicity. Continuous hydrolysis of DMMP in hot-compressed water is performed at temperatures from 200 to 300 °C, pressures of 20 and 30 MPa, and residence times from 30 to 80 s to evaluate the effects of pressure and temperature on reaction kinetics. DMMP hydrolysis is observed to follow pseudo-first-order reaction behavior, producing methylphosphonic acid and methanol as the only detectable reaction products. This is significant for the practical implementation of a continuous hydrothermal reactor for chemical warfare agent neutralization, as the process only yields stable, less-toxic compounds. Pressure has no discernible effect on the hydrolysis rate in compressed liquid water. Pseudo-first-order Arrhenius parameters are determined, with an activation energy of 90.17±5.68 kJ mol^{-1} and a pre-exponential factor of $10^{7.51\pm0.58}$ s^{-1}.

Keywords: Dimethyl Methylphosphonate, DMMP, Reaction Kinetics, Arrhenius, Hydrolysis, Chemical Warfare Agent

Introduction

Efforts are ongoing for the development of field-deployable processes or catalysts for rapid neutralization of high volumes of concentrated chemical warfare agents (CWAs) such as VX and GB. One possible process, alkaline hydrolysis, is currently being used to neutralize CWA stockpiles within the U.S. and abroad[1]. However, alkaline hydrolysis is typically performed at a central processing facility in a batch-type process, which is not well-suited for field deployment. The on-site decontamination of CWA stockpiles is a timely problem to address, and the adaption of hydrothermal treatment to a continuous reactor platform is a promising solution.

Hydrolysis of nerve agents yields a hydrolysate (*e.g.* VX/NaOH hydrolysate), which is less toxic, and does not require as stringent handling/processing requirements. The hydrolysate can be subsequently destroyed via an advanced oxidation process (AOP) such as radiolysis[2] or supercritical water oxidation (SCWO)[3]. While SCWO is highly effective for mineralizing CWAs and CWA hydrolysates, as evidenced by the current use of SCWO to process CWA hydrolysate at Blue Grass Chemical Agent-Destruction Pilot Plant in Kentucky[1, 4], no field-deployable SCWO platform has yet been developed. Challenges with miniaturizing components while adequately controlling reactor corrosion and clogging have hindered the development of a small-scale SCWO platform[4, 5].

VX ($C_{11}H_{26}NO_2PS$) and GB ($C_4H_{10}FO_2P$) are organophosphate CWAs which can be chemically simulated with less toxic organophosphates, such as dimethyl methylphosphonate (DMMP). DMMP ($C_3H_9O_3P$) is widely used as a simulant for investigating methods of detection, decontamination, and destruction of CWAs. DMMP has been used as a simulant to investigate the use of metal oxides[6-11], zeolites[12], and MOFs[13] to immobilize and destroy CWAs through

dissociative adsorption. There, the primary goal is to find a material that can adsorb and destroy airborne CWAs at ambient conditions, primarily for air filtration and treatment in a contaminated environment. While solid reagents are effective for CWA adsorption/decomposition, it is impractical to use them for destroying stockpiles of concentrated CWAs. A suitable thermochemical process is more practical for neutralizing high volumes of concentrated CWAs.

DMMP is known to rapidly hydrolyze at moderate temperatures (<300 °C) in water without the addition of a catalyst[3]. This process has a practical advantage for field deployment, as it only requires heat and water as inputs. Hot-compressed water is more straightforward to handle than supercritical water (SCW). It is less prone to the above-noted issues of corrosion and clogging. The rates of DMMP hydrolysis in hot-compressed water have not previously been reported, yet are required for the optimization of a continuous hydrolysis reactor.

This study quantifies the effects of temperature, pressure, and residence time on DMMP hydrolysis in a continuous water reactor without the addition of a catalyst. P-OCH_3 bond cleavage is expected as the favored DMMP hydrolysis mechanism[6-9]; the rates of P-OCH_3 bond cleavage determined in this study can reasonably be extrapolated to the hydrolysis of V- and G-type CWAs in liquid water at elevated temperatures and pressures. Previous studies[3, 14], show that methanol and methylphosphonic acid (MPA) are expected as stable end-products, following the global hydrolysis reaction:

$$C_3H_9O_3P + 2H_2O \rightarrow CH_5O_3P + 2CH_3OH$$

The initial DMMP concentration is low (5 wt%), thus the single-step reaction is expected to follow pseudo-first-order reaction kinetics. Arrhenius parameters are determined for the hydrolysis reaction from the pseudo-first-order reaction rates.

Materials and Methods

Experimental Apparatus. A continuous flow reactor is used for all experiments. Independently controlled HPLC pumps introduce cold reagent into a bulk flow of preheated water, to establish a clear reaction initiation point. A custom-fabricated mixing section is used to ensure rapid mixing and heating of the DMMP[15]. The mixing section introduces the reagent via four, axially symmetric 0.254 mm inner diameter (ID) injector ports into a central channel with a 3.05 mm ID.

After mixing, the reagents enter an Inconel 625 reactor section with an internal volume of 18.6 mL, and an internal surface-to-volume ratio of 13.1 cm^{-1}. As metal oxides are known to adsorb and decompose DMMP, it is possible that nickel-base reactor walls will catalyze the hydrolysis reaction to some degree. This simulates the operation and behavior of a practical reactor system. The reactor section is coiled to induce Dean vortices, ensuring reacting species are well-mixed throughout the reactor section. A radiant heater maintains isothermal conditions in the reactor section, verified by two Type-K thermocouples, downstream of which a heat exchanger rapidly quenches products to near-room temperatures. A reactor schematic is shown in Figure 1, and more information on reactor components and design methodology can be found elsewhere[5, 16].

Variation in reagent flow rates facilitates changes in reaction residence time, which is calculated based on the internal volume of the reactor, and the density of water at reaction conditions. A lack of tabulated densities for DMMP and MPA at experimental temperatures and pressures make a higher-precision determination of residence time challenging. As DMMP maximally comprises only 5 wt% of the mixture flowing through the reactor, and the density of DMMP at ambient conditions is 14.5% greater than the density of water, the use of water properties

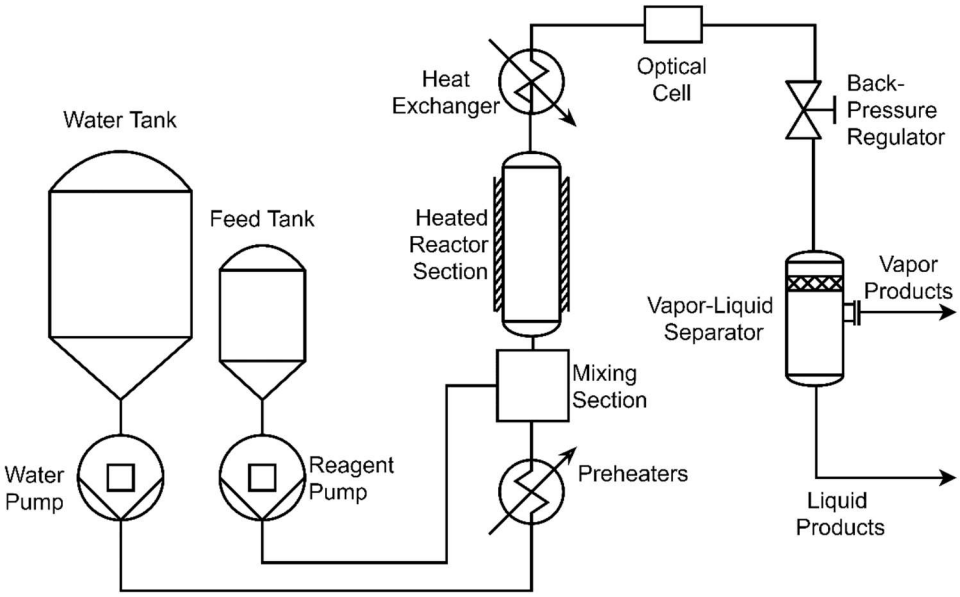

Figure 1. Schematic of continuous flow reactor used to conduct all experiments

is estimated to produce a maximum error of 0.7% in calculating the residence time. The reaction initiation point is defined as the point of reagent introduction, while the reaction termination point is defined as the inlet point to the heat exchanger. The flow path length between these locations is used to determine the internal reactor volume.

Reagent Purity and Preparation. DMMP (97%, Sigma-Aldrich) is used without further purification. An aqueous solution ($DMMP_{aq}$) of 50 wt% DMMP and 50 wt% deionized (DI) water is prepared and used for all experiments. $DMMP_{aq}$ is injected into preheated DI water at a 9:1 ratio of water:$DMMP_{aq}$ resulting in an overall initial DMMP concentration of 5 wt%.

Data Collection and Analysis. A high-resolution immersion Raman probe captures in-line spectra of product species in the quenched effluent stream, which are used to identify reactions products and quantify species concentrations in lieu of *ex situ* analysis methods such as high-pressure liquid chromatography (HPLC). Raman spectroscopy is well-suited to analyzing aqueous mixtures, as

water has a weak Raman signal, and its characteristic peaks can be used as an internal standard to aid with quantitative calibration.

A 785 nm Raman laser is operated at 300 mW in the backscatter configuration to collect spectral data. Five replicate spectra are collected for each experimental condition, with a spectral integration time of 20 s, to ensure steady-state operation, effluent homogeneity, and a low signal-to-noise ratio. The average of all five spectra is used to calculated product yields, while uncertainty in data collection is calculated from variance in the replicate spectra[17]. All products exist in a single liquid phase after quenching and are assumed to be well-mixed while passing through the interrogation volume of the Raman probe.

The subtraction of the fluorescent background signal resulting from the Raman spectrum of water is accomplished using a semi-automated baseline subtraction method[18]. Indirect hard modeling (IHM) is used to extract species concentration from collected Raman spectra[19, 20]. IHM facilitates quantitative analysis of overlapping Raman signals, via a weighted superposition of the pure spectra of constituent species. Quantitative calibration between Raman spectra and product concentrations is achieved via an indirect methodology described by Beumers et al.[21], where a least-square optimization of elemental balances between reactor inputs and outputs is used to perform calibration. For each pure compound, linear correlation between the spectral area and predicted species concentration is observed, verifying calibration accuracy. The pure Raman signals of all product species are determined by directly observing a species' Raman spectrum using the experimental setup. Figure 2 shows a representative Raman spectrum with the sapphire signal subtracted and peaks labeled. The wavenumbers of significant peaks are presented in Table 1.

Table 1. Species present in Raman spectra, with the wavenumbers of corresponding Raman peaks

Compound	Wavenumbers of Significant Raman Peaks (cm^{-1})
Sapphire (Al_2O_3)	379, 418, 751
Water (H_2O)	1640, 3185
DMMP ($C_3H_9O_3P$)	714, 1060, 2860, 2933, 2967
MPA (CH_5O_3P)	757, 2931
Methanol (CH_3OH)	1017, 1469, 2845, 2954

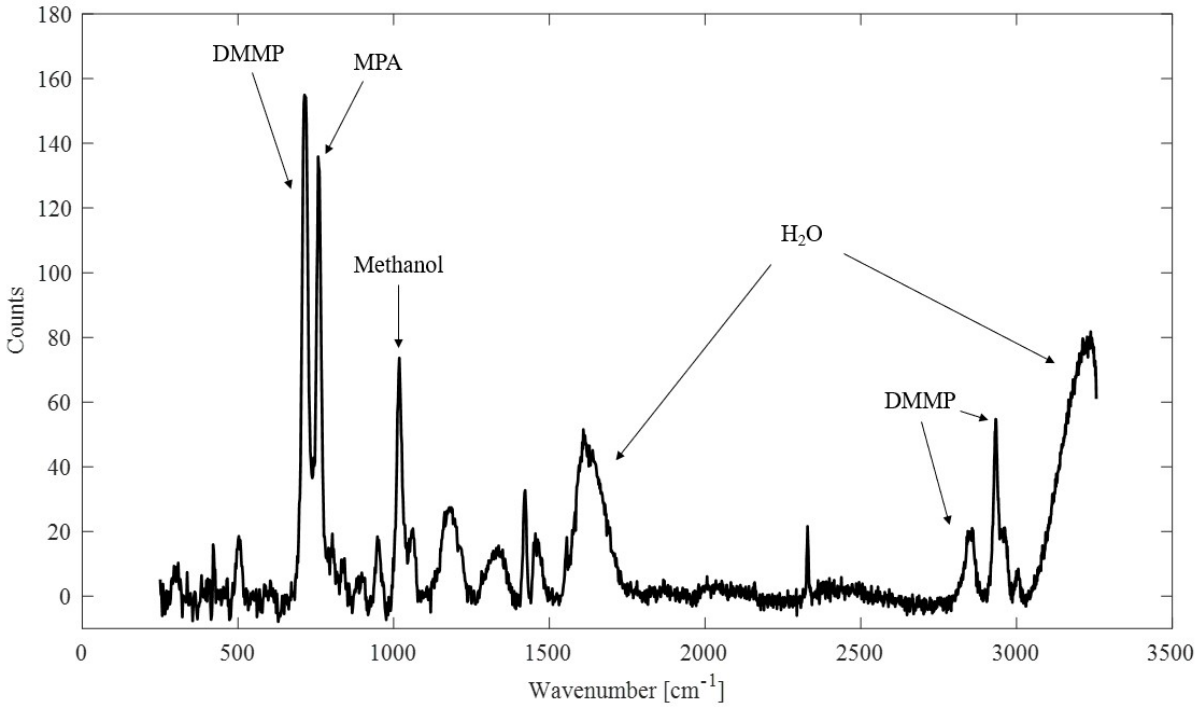

Figure 2. Representative Raman spectrum of DMMP hydrolysis products, with major peaks labelled. The sapphire signal (due to the optical window) is subtracted to clearly show the MPA peak at 757 cm^{-1}.

Determination of Reaction Rates and Rate Constants. DMMP has a strong and clearly visible Raman spectrum, and its yield can be reliably quantified in each experiment from the collected experimental spectra. It follows to use DMMP yield data to quantify the reaction rate constants at each temperature and pressure. With water abundantly present at a nearly constant concentration, and DMMP being the rate-limiting compound, the reaction can be assumed as pseudo-first-order with respect to DMMP[22].

Based on the pseudo-first-order assumption, the differential equation for temporal change in DMMP concentration can be expressed as:

$$\frac{d[DMMP]}{dt} = -k[DMMP]. \quad (1)$$

where k is the pseudo-first-order reaction rate constant. The corresponding time-dependent concentration expression is:

$$[DMMP] = [DMMP]_0 e^{-kt}, \quad (2)$$

where $[DMMP]_0$ is the initial molar DMMP concentration, and is set to unity to normalize data for ease of analysis. Similarly, the differential methanol concentration expression, based on the same rate constant and the global reaction stoichiometry, is:

$$\frac{d[MeOH]}{dt} = 2k[DMMP], \quad (3)$$

which can also be expressed as (substituting normalized Equation 2)

$$\frac{d[MeOH]}{dt} = 2ke^{-k} \ . \quad (4)$$

Solving this first-order differential equation yields a general expression for methanol concentration vs. time:

$$[MeOH] = 2 - 2e^{-k} \ . \quad (5)$$

Likewise, the general expression for MPA concentration vs. time, based on reaction stoichiometry is:

$$[MPA] = 1 - e^{-kt}. \quad (6)$$

k is determined for each experimental temperature and pressure by fitting Equation 2 to DMMP yield data. Predicted methanol and MPA concentration curves are generated and compared with experimental data in Figures 3 and 4.

Once k values are calculated for each temperature, the first-order Arrhenius parameters are determined using the global Arrhenius expression:

$$k = Ae^{-\frac{E_A}{RT}}, \tag{7}$$

where A is the pre-exponential factor and E_A is the activation energy. Both are determined by performing a linear curve fit between $\ln(k)$ and T^{-1}, using the modified form of the global Arrhenius expression:

$$\ln(k) = \ln(A) - \frac{E_A}{R}T^{-1}. \tag{8}$$

Experimental Conditions. The effect of temperature on reaction rate is evaluated by varying the experimental temperature from 200 to 300 °C at a constant pressure of 20 MPa. Pressure effects are tested by collecting data at 20 and 30 MPa and a temperature of 260 °C. Residence time is varied in 10 s increments from 30 to 80 s for each temperature and pressure.

Results & Discussion

Figure 3 shows product yields and product formation and decomposition profiles for each temperature tested at 20 MPa. DMMP hydrolysis follows a first-order decay profile. MPA and methanol are the only detected reaction products; no gaseous species are observed (*e.g.* H_2, CO, CO_2), nor is H_3PO_4 observed. Figure 4 shows no discernable effect of pressure change on the hydrolysis rate at 260 °C. Full DMMP decomposition is witnessed after 30 s at 300 °C. The two data points taken at 300 °C are not used to calculate a rate constant; instead, the experimentally determined Arrhenius parameters are used to simulate a decomposition curve at 300 °C, which predicts 99% DMMP conversion after 30 s, and 99.999% DMMP conversion after 58.9 s.

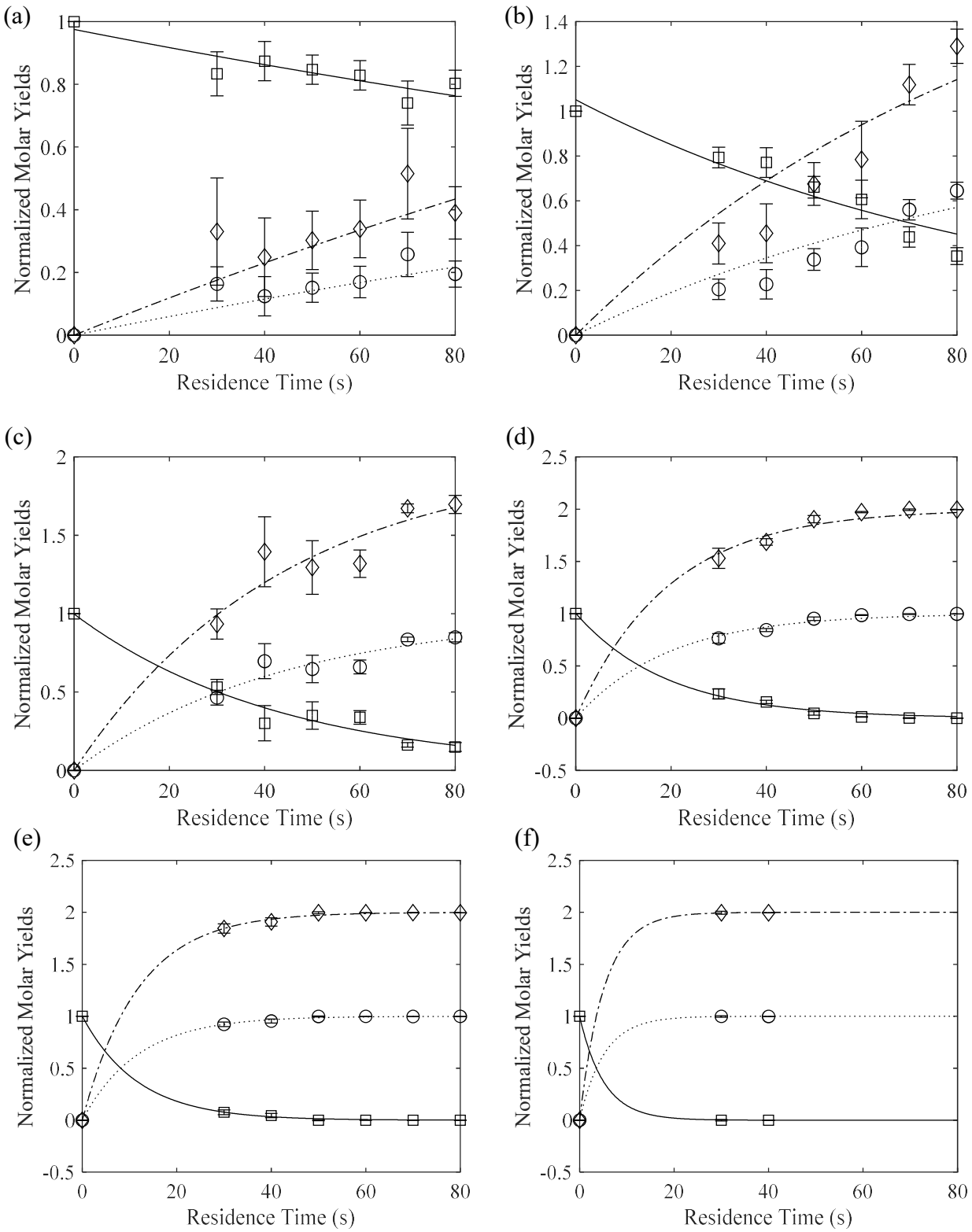

Figure 3. Product yields vs. residence time for DMMP (□–), MPA (○···), and methanol (◊-·-), at 20 MPa and (a) 200 °C, (b) 220 °C, (c) 240 °C, (d) 260 °C, (e) 280 °C and (f) 300 °C. Curves are generated from Equations 2, 5, and 6 using derived reaction rate (k) values. All values are normalized to 1 mol of initial DMMP

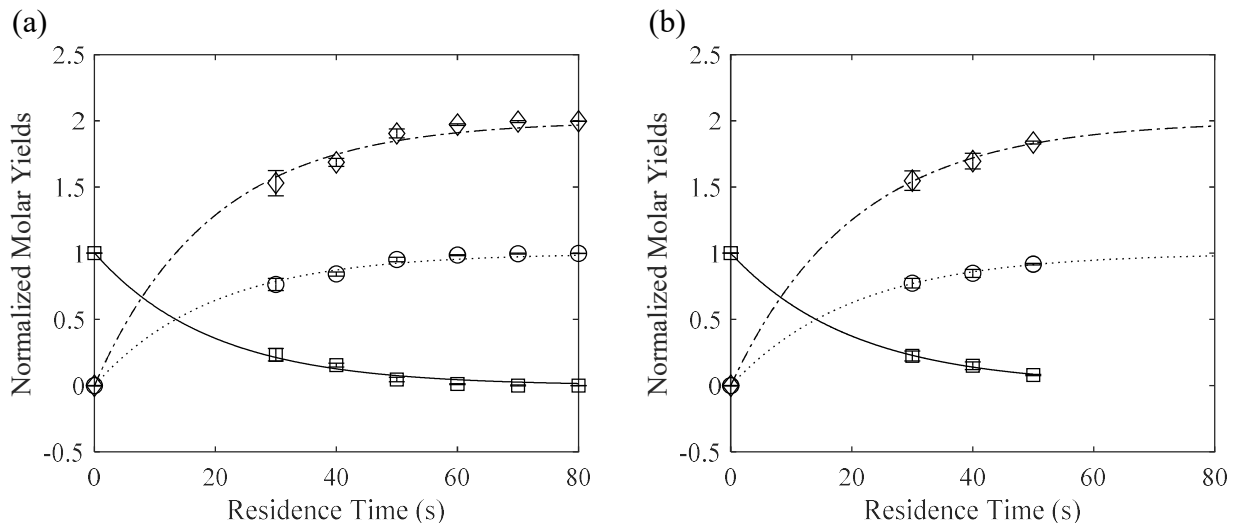

Figure 4. Product yields vs. residence time for DMMP (□–), MPA (○···), and methanol (◊-·-), at 260 °C and (a) 20 MPa and (b) 30 MPa. Curves are generated from Equations 2, 5, and 6 using derived reaction rate (k) values.

Kinetic Rates and Rate Parameters. Table 2 presents kinetic rates calculated from the DMMP decomposition observed at each experimental temperature and pressure. A temperature dependence is observed. However, pressure variation has a negligible effect on the reaction rate. Figure 5 shows an Arrhenius plot of hydrolysis rates vs. temperature for the range of temperatures that were tested. The kinetic rates follow a linear trend, confirming that the activation energy is constant for this reaction[22]. Fitting a trendline to the data following Equation 8 produces Arrhenius parameters of E_A = 90.17±5.68 kJ mol^{-1} and A = $10^{7.51\pm0.58}$ s^{-1} for the pseudo-first-order DMMP hydrolysis reaction, resulting in the global Arrhenius expression:

$$k = 10^{7.51\pm0.58} e^{-\frac{90.17\pm5.68\ kJ/mol}{RT}}\ s^{-1} \quad (9)$$

In our opinion, this Arrhenius expression is valid throughout the dense liquid phase. Should water experience a transition to the vapor or supercritical phase, these parameters would likely underestimate the reaction rate, as was demonstrated in the study of formic acid hydrolysis[16].

Table 2. Kinetic rates determined at each experimental temperature and pressure

Temperature (°C)	Pressure (MPa)	$k \cdot 10^{-2}$ (s^{-1})
200	20	0.31±0.18
220	20	1.06±0.40
240	20	2.29±0.56
260	20	5.17±0.79
260	30	4.91±0.40
280	20	8.52±1.99

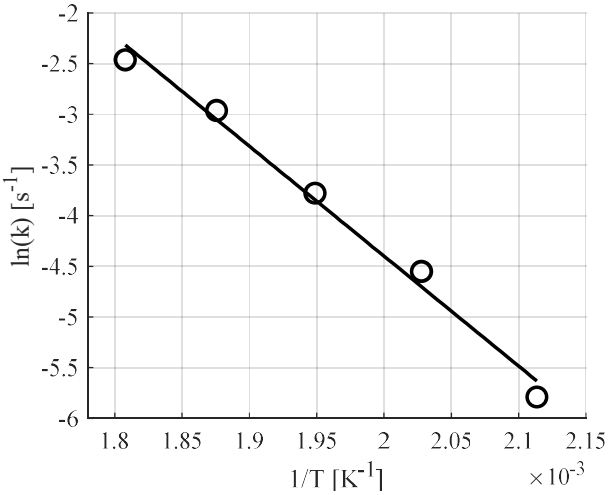

Figure 5. Arrhenius plot of DMMP hydrolysis reaction rates; linearity indicates that E_A is constant

Reactor Clogging. During preliminary testing, DMMP was introduced to a reactor bulk flow at 400 °C and 25 MPa - conditions above the critical point of water - with an initial concentration of 3 wt%. After running under these conditions for less than five minutes a clog formed in the reactor. The reactor was cooled overnight and purged using cold water; after that the reactor was fully operational.

It is likely that the blockage during operation at supercritical conditions was caused by the insolubility of phosphonates in supercritical water, and the precipitation of methylphosphonate on

the reactor walls[3]. Water becomes a nonpolar solvent above the critical point, and the solubility of most salts drops drastically, similar to the vapor phase of water. By operating below the critical point, the salt precipitation issue can be easily avoided.

As expected, no reactor blockage was observed during all experiments conducted at, or below, 300 °C. This confirms that hydrolysis of CWAs can be accomplished in hot-compressed water without the requirement of the advanced salt and/or heteroatom management strategies used in SCWO processes[4, 23-25]. This shows great promise towards the development of a simple, field-deployable CWA hydrolysis platform, requiring no inputs other than heat and water.

Conclusions

The reaction kinetics of DMMP hydrolysis in hot-compressed water are quantified. Arrhenius rate parameters are determined as E_A = 90.17±5.68 kJ mol^{-1} and A = $10^{7.51\pm0.58}$ s^{-1} for the pseudo-first-order DMMP hydrolysis reaction, with no observed pressure-dependency. Only MPA and methanol are observed as reaction products, which is significant for long term operational and practical implementation of a continuous hydrothermal approach for neutralization of CWAs. It is reasonable to assume that hydrolysis of G- and V-type nerve agents will follow similar reaction kinetic behavior in a continuous hot-compressed liquid water reactor, yielding stable, less-toxic products. The reported rate parameters can be used towards the design and optimization of a continuous platform for nerve agent hydrolysis.

AUTHOR INFORMATION

Corresponding Author

*pinkardb@uw.edu; +1 253 310-5882; ORCID: 0000-0002-4517-4712

Author Contributions

The manuscript was written through contributions of all authors. All authors have given approval to the final version of the manuscript.

Funding Sources

Funding for this work was by Defense Threat Reduction Agency (DTRA) - Grant HDTRA1-17-1-0001.

ACKNOWLEDGMENTs

Funding for this work was by Defense Threat Reduction Agency (DTRA) - Grant HDTRA1-17-1-0001. Special thanks to David Gorman and Kartik Tiwari for help with the initial design and fabrication of the reactor used for these experiments.

ABBREVIATIONS

AOP, advanced oxidation process; CWA, chemical warfare agent; DMMP, dimethyl methylphosphonate; $DMMP_{aq}$, 50 wt% aqueous DMMP; HPLC, high-pressure liquid chromatography; ID, inner diameter; MPA, methylphosphonic acid; SCWO, supercritical water oxidation

REFERENCES

(1) Centers for Disease Control and Prevention. Methods Used to Destroy Chemical Warfare Agents. https://www.cdc.gov/nceh/demil/methods.htm (accessed Dec 11, 2019).

(2) Aguila, A.; O'Shea, K. E.; Tobien T.; Asmus K. -D.; Reactions of Hydroxyl Radical with Dimethyl Methylphosphonate and Diethyl Methylphosphonate. A Fundamental Mechanistic Study. *J. Phys. Chem. A* **2001**, *105*, 7834-7839.

(3) Bianchetta, S.; Li, L.; Gloyna, E. F. Supercritical Water Oxidation of Methylphosphonic Acid. *Ind. Eng. Chem. Res.* **1999**, *38*, 2902-2910.

(4) National Academies of Sciences, Engineering, and Medicine. Metrics for Successful Supercritical Water Oxidation System Operation at the Blue Grass Chemical Agent Destruction Pilot Plant. *The National Academics Press*, Washington DC **2019**.

(5) Pinkard, B. R.; Gorman, D. J.; Tiwari, K.; Rasmussen, E. G.; Kramlich, J. C.; Reinhall, P. G.; Novosselov, I. V. Supercritical water gasification: practical design strategies and operational challenges for lab-scale, continuous flow reactors. *Heliyon* **2019**, *5*, e01269.

(6) Schweigert, I. V.; Gunlycke, D. Hydrolysis of Dimethyl Methylphosphonate by the Cyclic Tetramer of Zirconium Hydroxide. *J. Phys. Chem. A* **2017**, *121*, 7690-7696.

(7) Rusu, C. N.; Yates Jr., J. T. Adsorption and Decomposition of Dimethyl Methylphosphonate on TiO_2. *J. Phys. Chem. B* **2000**, *104*, 12292-12298.

(8) Gordon, W. O.; Tissue, B. M.; Morris, J. R. Adsorption and Decomposition of Dimethyl Methylphosphonate on Y_2O_3 Nanoparticles. *J. Phys. Chem. C* **2007**, *111*, 3233-3240.

(9) Mitchell, M. B.; Sheinker, V. N.; Mintz, E. A. Adsorption and Decomposition of Dimethyl Methylphosphonate on Metal Oxides. *J. Phys. Chem. B* **1997**, *101*, 11192-11203.

(10) Templeton, M. K.; Weinberg, W. H.; Adsorption and Decomposition of Dimethyl Methylphosphonate on an Aluminum Oxide Surface. *J. Am. Chem. Soc.* **1985**, *107*, 97-108.

(11) Li Y. -X.; Klabunde K. J.; Nanoscale Metal Oxide Particles as Chemical Reagents. Destructive Adsorption of a Chemical Agent Simulant, Dimethyl Methylphosphone, on Heat-Treated Magnesium Oxide. *Langmuir* **1991**, *7*, 1388-1393.

(12) Yang, S.; Doetchman, D. C.; Schulte, J. T.; Sambur, J. B.; Kanyi, C. W.; Fox, J. D.; Kowenje, C. O.; Jones, B. R.; Sherma, N. D. Sodium X-type faujasite zeolite decomposition of dimethyl methylphosphonate (DMMP) to methylphosphonate: Nucleophilic zeolite reactions I. *Microporous Mesoporous Mater.* **2006**, *92*, 56-60.

(13) Ma, F. -J.; Liu, S. -X.; Sun C. -Y.; Liang D. -D.; Ren G. -J.; Wei F.; Chen Y. -G.; Su Z. -M.; A Sodalite-Type Porous Metal-Organic Framework with Polyoxometalate Templates: Adsorption and Decomposition of Dimethyl Methylphosphonate. *J. Am. Chem. Soc.* **2011**, *133*, 4178-4181.

(14) Pinkard, B. R.; Kramlich, J. C.; Novosselov, I. V. Gasification Pathways and Reaction Mechanisms of Primary Alcohols in Supercritical Water. *ACS Sus. Chem. Eng.* **2020**, *8*, 4598-4605.

(15) Tiwari, K.; Pinkard, B. R.; Gorman, D. J.; Davis, J.; Kramlich, J. C.; Reinhall, P. G.; Novosselov, I. V. Computational modeling of mixing and gasification in continuous-flow supercritical water reactor. In: *Proceedings of the 12th International Symposium on Supercritical Fluids* **2018**.

(16) Pinkard, B. R.; Gorman, D. J.; Rasmussen, E. G.; Kramlich, J. C.; Reinhall, P. G.; Novosselov, I. V. Kinetics of formic acid decomposition in subcritical and supercritical water - a Raman Spectroscopic study. *Int. J. Hydrog. Energy* **2019**, *44*, 31745-31756.

(17) Pelletier, M. J.; Quantitative analysis using Raman spectroscopy. *Appl. Spectrosc.* **2003**, *57*, 20A-42A.

(18) Pinkard, B. R.; Gorman, D. J.; Rasmussen, E. G.; Maheshwari, V.; Kramlich, J. C.; Reinhall, P. G.; Novosselov, I. V. Raman Spectroscopic Data from Formic Acid Decomposition in Subcritical and Supercritical Water. *Data Brief* **2020**, *29*, 105312.

(19) Kriesten, E.; Alsmeyer, F.; Bardow, A.; Marquardt, W. Fully automated indirect hard modeling of mixture spectra. *Chemom. Intell. Lab. Syst.* **2008**, *91*, 181-193.

(20) Alsmeyer, F.; Koss, H. J.; Marquardt, W. Indirect spectral hard modeling for the analysis of reactive and interacting mixtures. *Appl. Spectrosc*. **2004**, *58*, 975-985.

(21) Beumers, P.; Brands, T.; Koss, H. J.; Bardow, A. Model-free calibration of Raman measurements of reactive systems: Application to monoethanolamine/water/CO_2. *Fluid Phase Equilib.* **2016**, *424*, 52-57.

(22) Helfferich, F. G. *Kinetics of homogeneous multistep reactions*. Elsevier, **2001**.

(23) Bermejo, M. D.; Cocero, M. J. Destruction of an industrial wastewater by supercritical water oxidation in a transpiring wall reactor. *J. Haz. Mat.* **2006**, *137*, 965-971.

(24) Serikawa, R. M.; Usui, T.; Nishimura, T.; Sato, H.; Hamada, S.; Sekino, H. Hydrothermal flames in supercritical water oxidation: investigation in a pilot scale continuous reactor. *Fuel* **2002**, *81*, 1147-1159.

(25) Bermejo, M. D.; Rincon, D.; Martin, A.; Cocero, M. J. Experimental performance and modeling of a new cooled-wall reactor for the supercritical water oxidation. *Ind. Eng. Chem. Res.* **2009**, *48*, 6262-6272.